

Debiased Graph Contrastive Learning

Jun Xia^{1, 2, 3}, Lirong Wu^{2, 3}, Jintao Chen¹, Ge Wang^{2, 3}, Stan Z. Li^{2, 3}*

¹ Zhejiang University

² School of Engineering, Westlake University

³ Institute of Advanced Technology, Westlake Institute for Advanced Study
{xiajun, wulirong, wangge, stan.zq.li}@westlake.edu.cn, chenjintao@zju.edu.cn

Abstract

Contrastive learning (CL) has emerged as a dominant technique for unsupervised representation learning which embeds augmented versions of the anchor close to each other (positive samples) and pushes the embeddings of other samples (negative samples) apart. As revealed in recent works, CL can benefit from hard negative samples (negative samples that are difficult to distinguish from the anchor). However, we observe minor improvement or even performance drop when we adopt existing hard negative mining techniques in Graph Contrastive Learning (GCL). We find that many hard negative samples similar to anchor point are false negative ones (samples from the same class as anchor point) in GCL, which is different from CL in computer vision and will lead to unsatisfactory performance of existing hard negative mining techniques in GCL. To eliminate this bias, we propose Debiased Graph Contrastive Learning (DGCL), a novel and effective method to estimate the probability whether each negative sample is true or not. With this probability, we devise two schemes (i.e., DGCL-weight and DGCL-mix) to boost the performance of GCL. Empirically, DGCL outperforms or matches previous unsupervised state-of-the-art results on several benchmarks and even exceeds the performance of supervised ones. The code for reproducing the results can be found in the supplementary materials.

Introduction

Graph representation learning with Graph Neural Networks (GNNs) has become a prominent technique to learn a low-dimensional embedding that preserves structure information. However, most existing GNNs are trained in a supervised manner and it is often resource- and time-intensive to collect abundant labeled data (Xia et al. 2021). Recently, contrastive learning (CL) has demonstrated unprecedented unsupervised performance in computer vision (He et al. 2020; Chen et al. 2020), natural language processing (Gao, Yao, and Chen 2021) and graph representation learning (Velickovic et al. 2019; Hassani and Khasahmadi 2020; Zhu et al. 2021b).

As with metric learning, recent works both theoretically and practically validate that hard negative samples con-

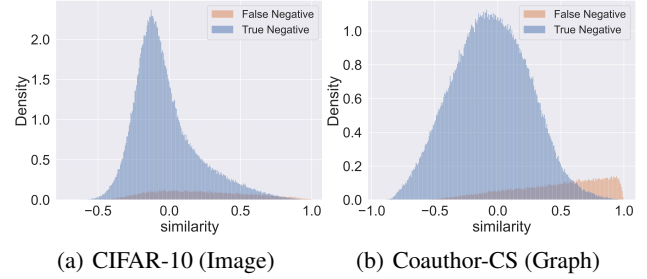


Figure 1: Similarity histograms of negative samples. Here similarity refers to cosine similarity between normalized embeddings of anchor and negative sample. we take CIFAR-10 and Coauthor-CS as examples. For CIFAR-10, we adopt SimCLR (Chen et al. 2020) framework. For GCL, we adopt GCA (Zhu et al. 2021b). False (True) Negatives refer to samples that are (or not) from the same class with the anchor. More examples can be found in Figure 3 and the appendix.

tribute more to CL. For example, HCL (Robinson et al. 2021) develops a family of unsupervised sampling methods for selecting hard negative samples and MoCHi (Kalantidis et al. 2020) mixes the hard negative samples to synthesize more hard negative ones. However, we observe minor improvement or even performance drop when we adopt these negative mining techniques in GCL (the results can be seen in Table 5). Concurrent to our work, (Zhu et al. 2021a) also observes that existing hard negative mining techniques that work well in other domains bring limited benefits to GCL. Unfortunately, they don’t provide any solution to tackle this issue. To explain these phenomena, we first plot the negative samples distributions over similarity of various datasets in Figure 1. Please kindly note that we do not observe significant changes of negative samples distribution in the training process of SimCLR (Chen et al. 2020) on CIFAR-10 and other image datasets. However, for GCL, the negative samples distribution is bimodal for a long period and then progressively transit to unimodal distribution. Similar phenomena for more datasets can be found in the appendix. These provide explanations for the poor performance of existing negative mining techniques in GCL. Specifically, they regard the negative samples that are most similar to anchor points as hard ones. However, as can be observed in Figure 1(b), many “hard” ones are false negative samples in

*Corresponding author
Preprint.

GCL indeed, which is different from CL in computer vision and will undesirably push away the semantically similar samples. The existence of false negatives is termed as *sampling bias* in Debaised Contrastive Learning (DCL) (Chuang et al. 2020). However, as reported in Table 5 and (Zhu et al. 2021a), DCL brings performance drop for GCL because the sampling bias is severer in GCL. Now, we are naturally motivated to ask following question: *Can we devise a more suitable method to eliminate severer sampling bias for GCL?*

To answer this question, we argue that true and false negatives can be distinguished by fitting a two-component (true-false) beta mixture model (BMM) on the similarity. The posterior probabilities under the model can be utilized to weight the negative samples properly and synthesize more true hard negative samples for performance improvement. We highlight the following contributions:

- We demonstrate the difference between GCL and previous CL and explain why existing techniques which emphasize hard negative samples can not work well in GCL.
- We propose to utilize BMM to estimate the probability whether each negative sample is true or not.
- With the posterior probabilities under the model, we devise two schemes (i.e., DGCL-weight and DGCL-mix) to boost GCL.
- DGCL outperforms or matches the previous unsupervised state-of-the-art results on multiple graph benchmarks and even exceeds the performance of supervised ones.

Related Work

Contrastive Learning (CL). CL has achieved immense success in unsupervised representation learning. Generally, most CL frameworks treat any two samples in the dataset as negative pairs and meanwhile establish positive pairs by combing the samples with their perturbation (Wu et al. 2018; Chen et al. 2020; He et al. 2020). It has been theoretically and practically validated that harder negative samples will boost the performance of CL (Ho and Vasconcelos 2020; Kalantidis et al. 2020; Hu et al. 2020). With this motivation, HCL (Robinson et al. 2021) develops a new family of unsupervised sampling methods for selecting hard negative samples. Moreover, MoChi (Kalantidis et al. 2020) selects samples which are most similar to anchor points as hard negative ones and then mixes them to synthesize more hard negative samples and Ring (Wu et al. 2021b) introduces a family of mutual information estimators that sample negatives in a “ring” around each positive. However, as shown in Table 5, these techniques which emphasize hard negative samples don’t work well in GCL.

Unsupervised Graph Representation Learning. Initially, vast majority of traditional methods for unsupervised graph representation learning forces neighboring nodes to have similar embeddings. For example, DeepWalk (Perozzi, Al-Rfou, and Skiena 2014) and node2vec (Grover and Leskovec 2016) regard nodes appearing in the same random walk as positive samples. However, they have been proved to overly emphasize on the encoded structural information (Qiu et al. 2018). Recently, with the prosperity of Graph Neural Networks (GNNs), unsupervised graph representation learning

has adopted more powerful GNNs as the encoder and decoder. Prototypical examples are Graph AutoEncoder and its advanced versions (Kipf and Welling 2016b; Pan et al. 2018), they learn graph embedding utilizing reconstruction loss. However, these generative methods incline to obtain less discriminative representation. Another line of works follow contrastive paradigm. For example, DGI (Velickovic et al. 2019) proposes to maximize the mutual information between graph-level and node-level embeddings. Similarly, GMI (Peng et al. 2020) adopts two discriminators to directly measure mutual information between input and representations of both nodes and edges. Besides, MVGRL (Hassani and Khasahmadi 2020) proposes to learn both node-level and graph-level representation by performing node diffusion and contrasting node representation to augmented graph representation. Different from our work, GraphCL (You et al. 2020) adopts SimCLR framework and define four data augmentations for graph-level representation learning. More recently, GRACE (Zhu et al. 2020) maximizes the agreement of node embeddings across two corrupted views of the graph. Furthermore, GCA (Zhu et al. 2021b) equips GRACE with adaptive data augmentation that preserving intrinsic structures and attributes when augmenting graph data. We recommend readers to refer to a recent review of more relevant literature (Wu et al. 2021a). In this paper, we consider hard negatives and sampling bias to further boost existing GCL frameworks such as GCA and GRACE on node-level representation learning task, which has been seldomly explored in GCL.

Methodology

Preliminaries

Let $\mathcal{G} = (\mathcal{V}, \mathcal{E})$ be the graph, where $\mathcal{V} = \{v_1, v_2, \dots, v_N\}$, $\mathcal{E} \subseteq \mathcal{V} \times \mathcal{V}$ denote the node set and edge set respectively. Besides, $\mathbf{X} \in \mathbb{R}^{N \times F}$ and $\mathbf{A} \in \{0, 1\}^{N \times N}$ are the feature matrix and the adjacency matrix respectively. $\mathbf{x}_i \in \mathbb{R}^F$ is the feature of v_i , and $\mathbf{A}_{ij} = 1$ iff $(v_i, v_j) \in \mathcal{E}$. Our objective is to learn a GNN encoder $f(\mathbf{X}, \mathbf{A}) \in \mathbb{R}^{N \times F'}$ to embed nodes in low dimensional space in absence of label information, i.e. $F' \ll F$. These low dimensional representations can be used in downstream tasks, such as node classification.

Graph Contrastive Frameworks

We first introduce existing graph contrastive frameworks GCA and GRACE below. Similar to SimCLR (Chen et al. 2020), they sample two augmentation functions $t \sim \mathcal{T}$ and $t' \sim \mathcal{T}$, here \mathcal{T} is the set of all augmentation functions. The augmentations are uniform and adaptive for GRACE and GCA respectively. Then, we can obtain two views for the graph, i.e., $\tilde{\mathcal{G}}_1 = t(\mathcal{G})$ and $\tilde{\mathcal{G}}_2 = t'(\mathcal{G})$. Given that $\tilde{\mathcal{G}}_1 = (\tilde{\mathbf{X}}_1, \tilde{\mathbf{A}}_1)$ and $\tilde{\mathcal{G}}_2 = (\tilde{\mathbf{X}}_2, \tilde{\mathbf{A}}_2)$, We can then denote node embeddings in the two views as $\mathbf{U} = f(\tilde{\mathbf{X}}_1, \tilde{\mathbf{A}}_1)$ and $\mathbf{V} = f(\tilde{\mathbf{X}}_2, \tilde{\mathbf{A}}_2)$. For any node v_i , its embedding in one view v_i is regarded as the anchor. The embedding \mathbf{u}_i in the other view is the positive sample and the embeddings of other nodes in both views are negative samples. Similar to

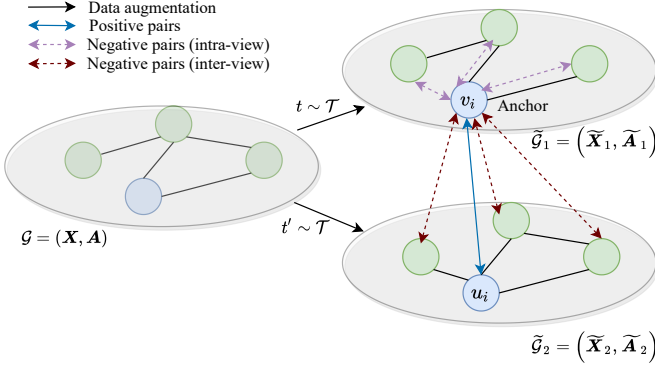


Figure 2: Overview of the GCL framework in (Zhu et al. 2020; 2021b).

the InfoNCE objective used in computer vision, they define the training objective for each positive pair (u_i, v_i) as,

$$\ell(u_i, v_i) = \log \frac{e^{\theta(u_i, v_i)/\tau}}{\underbrace{e^{\theta(u_i, v_i)/\tau}}_{\text{positive pair}} + \underbrace{\sum_{k \neq i} e^{\theta(u_i, v_k)/\tau}}_{\text{inter-view negative pairs}} + \underbrace{\sum_{k \neq i} e^{\theta(u_i, u_k)/\tau}}_{\text{intra-view negative pairs}}}, \quad (1)$$

where the critic $\theta(u, v) = s(g(u), g(v))$. Here $s(\cdot, \cdot)$ is the cos similarity and $g(\cdot)$ is linear projection to enhance the expression power of the critic function (Tschannen et al. 2019; Chen et al. 2020). In practice, g is implemented with a two-layer perceptron model. With the symmetry of the two views, we can then define the overall loss as the average of all the positive pairs,

$$\mathcal{J} = -\frac{1}{2N} \sum_{i=1}^N [\ell(u_i, v_i) + \ell(v_i, u_i)]. \quad (2)$$

Debiased Graph Contrastive Learning

We aim to estimate the probability whether each negative sample is true or not. As can be observed in Figure 3, there is a significant difference between the false negative and true negative samples' distribution in GCL, allowing the two types of samples can be distinguished from the similarity distribution. Here we propose to utilize mixture model to estimate the probability.

Mixture models are popular unsupervised modeling techniques (Lindsay 1995; Everitt 2014), among which Gaussian Mixture Model (GMM) (Ji et al. 2017; Lee et al. 2021) is the most popular one. However, as can be observed in Figure 3, the distribution of false negative samples is skew and thus symmetric Gaussian distribution can not fit this well. To circumvent this issue, we resort to Beta Mixture Model (BMM) (Ji et al. 2005) which is flexible enough to model various distributions (symmetric, skewed, arched distributions and so on) over $[0, 1]$. As can be observed in Figure 3,

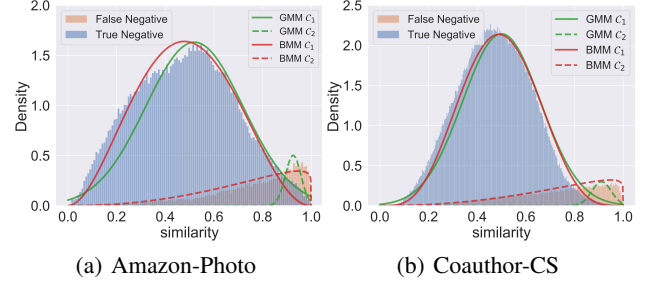


Figure 3: Empirical distribution and estimated GMM and BMM on Amazon-Photo and Coauthor-CS datasets. The BMM fits the distributions better. Here $\mathcal{C}_1, \mathcal{C}_2$ denote the estimated distributions of two components respectively. We provide results on more datasets in the appendix.

BMM can fit the empirical distribution better than GMM and we provide examples on more datasets in the appendix. Also, we compare the performance of DGCL with BMM and GMM in Table 4 and find that BMM consistently outperforms GMM. The probability density function (pdf) of beta distribution is,

$$p(s | \alpha, \beta) = \frac{\Gamma(\alpha + \beta)}{\Gamma(\alpha)\Gamma(\beta)} s^{\alpha-1} (1-s)^{\beta-1}, \quad (3)$$

where $\alpha, \beta > 0$ are the parameters of beta distribution and $\Gamma(\cdot)$ is gamma function. The pdf of beta mixture model of C components on s (Min-Max normalized cosine similarity between normalized embeddings of anchor and negative sample) can be defined as:

$$p(s) = \sum_{c=1}^C \lambda_c p(s | \alpha_c, \beta_c), \quad (4)$$

where λ_c are the mixture coefficients for convex combination of each individual beta distribution. Here we can fit a two-component GMM (i.e., $C = 2$) to model the distribution of true and false negative samples. We then utilize Expectation Maximization (EM) algorithm to fit BMM to the observed distribution. In the E-step, we fix the parameters of BMM $(\lambda_c, \alpha_c, \beta_c)$ and update $p(c | s)$ with Bayes rule,

$$p(c | s) = \frac{\lambda_c p(s | \alpha_c, \beta_c)}{\sum_{j=1}^C \lambda_j p(s | \alpha_j, \beta_j)}. \quad (5)$$

In practice, fitting BMM with all the similarities will incur high computational cost. Instead, we can fit BMM well by only sampling M ($M \ll N^2$) similarities for simplification. Larger M bring limited benefits, which we will validate in the appendix. We can then obtain the weighted average \bar{s}_c and variance v_c^2 over M similarities,

$$\bar{s}_c = \frac{\sum_{i=1}^M p(c | s_i) s_i}{\sum_{i=1}^M p(c | s_i)}, \quad (6)$$

$$v_c^2 = \frac{\sum_{i=1}^M p(c | s_i) (s_i - \bar{s}_c)^2}{\sum_{i=1}^M p(c | s_i)}. \quad (7)$$

For M-step, the component model parameters α_c, β_c can be estimated using the method of moments in statistics,

$$\alpha_c = \bar{s}_c \left(\frac{\bar{s}_c (1 - \bar{s}_c)}{v_c^2} - 1 \right), \quad (8)$$

$$\beta_c = \frac{\alpha_c (1 - \bar{s}_c)}{\bar{s}_c}, \quad (9)$$

and coefficients λ_c for mixing can be calculated as,

$$\lambda_c = \frac{1}{M} \sum_{i=1}^M p(c | s_i), \quad (10)$$

The above E and M-steps are iterated until convergence or the maximum of iterations I are reached. In our experiments, we set $I = 10$. Finally, we can obtain the probability of a sample being true or false negative with the posterior probability with the similarity s_i ,

$$p(c | s_i) = \frac{p(c)p(s_i | \alpha_c, \beta_c)}{p(s_i)}, \quad (11)$$

where $c = 0$ or $c = 1$ corresponds to true or false negative respectively.

Remark: Computational Overhead

It is noteworthy that the estimation of the posterior probabilities introduces light computational overhead. Firstly, we only have to fit BMM once during the training process instead of once per epoch. Secondly, we can fit BMM well with M ($M \ll N^2$) similarities and the time complexity of EM algorithm for fitting in DGCL is $\mathcal{O}(IM)$. I is the maximum of iterations. Thirdly, we only have to fit BMM with similarities from single view because both inter-view and intra-view include all negative pairs. In our experiments, we only utilize similarities from inter-view to fit BMM.

Two schemes for boosting GCL

With the posterior probabilities, we devise two schemes to boost the performance of existing GCL. We introduce them in details below.

Scheme 1: DGCL-weight

As revealed above, GCL suffers from severe sampling bias which will undermine the performance. To tackle this problem, we propose to allocate more weights for the samples that are more likely to be true negative ones,

$$\ell_w(\mathbf{u}_i, \mathbf{v}_i) = \log \frac{e^{\frac{\theta(\mathbf{u}_i, \mathbf{v}_i)}{\tau}}}{\underbrace{e^{\frac{\theta(\mathbf{u}_i, \mathbf{v}_i)}{\tau}}}_{\text{positive pair}} + \underbrace{\sum_{k \neq i} w(i, k) e^{\frac{\theta(\mathbf{u}_i, \mathbf{v}_k)}{\tau}}}_{\text{inter-view negative pairs}} + \underbrace{\sum_{k \neq i} w(i, k) e^{\frac{\theta(\mathbf{u}_i, \mathbf{u}_k)}{\tau}}}_{\text{intra-view negative pairs}}}, \quad (12)$$

$$w(i, k) = \frac{p(0 | s_{ik})}{\frac{1}{N-1} \sum_{j \neq i} p(0 | s_{ij})}, \quad (13)$$

where s_{ik} is the similarity between anchor \mathbf{u}_i and its inter-view negative sample \mathbf{v}_k . Note $w(i, k)$ can be utilized to

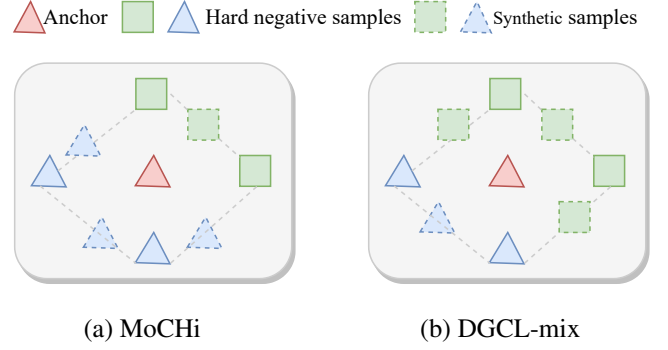


Figure 4: Comparison between MoCHi (Kalantidis et al. 2020) and DGCL-mix. Gray dotted lines denote mixing and the classes are distinguished by the shapes of samples. DGCL-mix synthesizes more true negative samples.

weight both inter-view ($\mathbf{u}_i, \mathbf{v}_k$) and intra-view ($\mathbf{u}_i, \mathbf{u}_k$) negative pair. We can then define the new overall loss as the average of all the positive pairs,

$$\mathcal{J}_w = -\frac{1}{2N} \sum_{i=1}^N [\ell_w(\mathbf{u}_i, \mathbf{v}_i) + \ell_w(\mathbf{v}_i, \mathbf{u}_i)] \quad (14)$$

Scheme 2: DGCL-mix

Recently, MoCHi (Kalantidis et al. 2020) proposes hard negative mixing strategies to synthesize more hard negative samples. However, as analysed above, many synthesized samples in GCL are positive samples indeed, which will deteriorate the performance. To remedy this deficiency, we propose DGCL-mix which synthesizes more hard negative samples considering the probability whether the negative samples are true ones or not. The comparison between MoCHi and DGCL-mix can be seen in Figure 4. More specifically, for each anchor point \mathbf{u}_i , we synthesize m hard negative samples by convex linear combinations of pairs of its “hardest” existing negatives. Here, “hardest” existing negatives refers to N' samples that are most similar to the anchor point. Instead of mixing N' samples randomly, we mixing them by emphasizing samples that are more likely to be true negative. Formally, for each anchor \mathbf{u}_i , a synthetic point $\tilde{\mathbf{u}}_k$ ($k \in [1, m]$) would be given by,

$$\tilde{\mathbf{u}}_k = \alpha_k \mathbf{v}_p + (1 - \alpha_k) \mathbf{v}_q, \quad (15)$$

where $\mathbf{v}_p, \mathbf{v}_q$ are selected from N' “hardest” existing negatives and α_k can be calculated as,

$$\alpha_k = \frac{p(0 | s_{ip})}{p(0 | s_{ip}) + p(0 | s_{iq})}, \quad (16)$$

we can then define the training objective for each positive pair ($\mathbf{u}_i, \mathbf{v}_i$) with the synthetic negatives,

$$\ell_m(\mathbf{u}_i, \mathbf{v}_i) = \log \frac{e^{\frac{\theta(\mathbf{u}_i, \mathbf{v}_i)}{\tau}}}{\underbrace{e^{\frac{\theta(\mathbf{u}_i, \mathbf{v}_i)}{\tau}}}_{\text{positive pair}} + \underbrace{\sum_{k \neq i} e^{\frac{\theta(\mathbf{u}_i, \mathbf{v}_k)}{\tau}}}_{\text{inter-view negative pairs}} + \underbrace{\sum_{k \neq i} e^{\frac{\theta(\mathbf{u}_i, \mathbf{u}_k)}{\tau}}}_{\text{intra-view negative pairs}} + \underbrace{\sum_{k=1}^m e^{\frac{\theta(\mathbf{u}_i, \tilde{\mathbf{u}}_k)}{\tau}}}_{\text{synthetic negative pairs}}}. \quad (17)$$

Note that we synthesize new samples only with inter-view hard negatives. Although synthesizing more samples with intra-view hard negatives may help, we validate the improvement is limited while introducing unnecessary computational overhead in the appendix. Finally, we can define the new overall loss,

$$\mathcal{J}_m = -\frac{1}{2N} \sum_{i=1}^N [\ell_m(\mathbf{u}_i, \mathbf{v}_i) + \ell_m(\mathbf{v}_i, \mathbf{u}_i)]. \quad (18)$$

The training algorithms of both DGCL-weight and DGCL-mix for transductive tasks are summarized in Algorithm 1. The algorithm for inductive tasks can be found in the appendix for the limited space.

Algorithm 1 DGCL-weight & DGCL-mix (Transductive)

Input: $\mathcal{T}, \mathcal{G}, f, g, N$, normalized cosine similarity s , epoch for fitting BMM E , *mode* (‘weight’ or ‘mix’).
for $epoch = 0, 1, 2, \dots$ **do**
 Draw two augmentation functions $t \sim \mathcal{T}, t' \sim \mathcal{T}$
 $\hat{\mathcal{G}}_1 = t(\mathcal{G}), \hat{\mathcal{G}}_2 = t'(\mathcal{G});$ \triangleright Augmentation.
 $\mathcal{U} = f(\hat{\mathcal{G}}_1), \mathcal{V} = f(\hat{\mathcal{G}}_2);$ \triangleright Embedding.
 for $\mathbf{u}_i \in \mathcal{U}$ and $\mathbf{v}_i \in \mathcal{V}$ **do**
 $s_{ij} = s(g(\mathbf{u}_i), g(\mathbf{v}_i))$ \triangleright Similarity.
 if $epoch = E$ **then** \triangleright Fitting BMM.
 Compute $p(0 | s_{ij})$ with Eq. (4) to Eq. (11).
 end if
 end for
 if $epoch \geq E$ **then**
 if $mode = \text{‘weight’}$ **then** \triangleright DGCL-weight
 Compute \mathcal{J}_w with Eq. (12) to Eq. (14).
 Update the parameters of f, g with \mathcal{J}_w .
 end if
 if $mode = \text{‘mix’}$ **then** \triangleright DGCL-mix
 Compute \mathcal{J}_m with Eq. (15) to Eq. (18).
 Update the parameters of f, g with \mathcal{J}_m .
 end if
 else \triangleright GCL
 Compute \mathcal{J} with Eq. (1) to Eq. (2).
 Update the parameters of f, g with \mathcal{J} .
 end if
end for
Output: f, g .

Experiments

In this section, we empirically assess the quality of produced node representations on transductive and inductive node classification tasks using six public benchmark datasets.

Experimental Setup & Baselines

Following previous works (Velickovic et al. 2019; Zhu et al. 2020), we first train the model in an unsupervised manner. Then, the resulting embeddings are utilized to train and test a simple ℓ_2 -regularized logistic classifier. We train the classifier for 20 runs. Besides, we adopt GRACE framework and measure performance using micro-averaged F1-score on

inductive tasks. For transductive tasks, we adopt GCA and report the test accuracy.

Transductive learning. We adopt a two-layer GCN (Kipf and Welling 2016a) as the encoder for transductive learning following previous works (Velickovic et al. 2019; Zhu et al. 2020). We can describe the architecture of the encoder as,

$$\begin{aligned} \text{GC}_i(\mathbf{X}, \mathbf{A}) &= \sigma \left(\hat{\mathbf{D}}^{-\frac{1}{2}} \hat{\mathbf{A}} \hat{\mathbf{D}}^{-\frac{1}{2}} \mathbf{X} \mathbf{W}_i \right), \\ f(\mathbf{X}, \mathbf{A}) &= \text{GC}_2(\text{GC}_1(\mathbf{X}, \mathbf{A}), \mathbf{A}), \end{aligned} \quad (19)$$

where $\hat{\mathbf{A}} = \mathbf{A} + \mathbf{I}$ is the adjacency matrix with self-loops and $\hat{\mathbf{D}} = \sum_i \hat{\mathbf{A}}_i$ is the degree matrix, $\sigma(\cdot)$ is a nonlinear activation function. \mathbf{W}_i is the learnable weight matrix.

We consider our DGCL with multiple baselines including traditional methods DeepWalk (Perozzi, Al-Rfou, and Skiena 2014) and node2vec (Grover and Leskovec 2016). Besides, we also consider other deep learning based methods including Graph AutoEncoders (GAE, VGAE) (Kipf and Welling 2016b), Deep Graph Infomax (DGI) (Velickovic et al. 2019), Graphical Mutual Information Maximization (GMI) (Peng et al. 2020), Multi-View Graph Representation Learning (MVGRL) (Hassani and Khasahmadi 2020), negative-sample-free method (BGRL) (Thakoor et al. 2021) and GCL with adaptive augmentations (GCA) (Zhu et al. 2021b). We report the best performance of three variants of GCA. We also compare DGCL with supervised counterparts including two representative models Graph Convolutional Networks (GCN) (Kipf and Welling 2016a) and Graph Attention Networks (GAT) (Velićković et al. 2017).

Inductive learning on large graphs. Considering the large scale of some graph datasets, we adopt a three-layer GraphSAGE-GCN (Hamilton, Ying, and Leskovec 2017) with residual connections (He et al. 2016) as the encoder following DGI (Velickovic et al. 2019) and GRACE (Zhu et al. 2020). The architecture of the encoder can be formulated as,

$$\begin{aligned} \widehat{\text{MP}}_i(\mathbf{X}, \mathbf{A}) &= \sigma \left(\left[\hat{\mathbf{D}}^{-1} \hat{\mathbf{A}} \mathbf{X}; \mathbf{X} \right] \mathbf{W}_i \right), \\ f(\mathbf{X}, \mathbf{A}) &= \widehat{\text{MP}}_3 \left(\widehat{\text{MP}}_2 \left(\widehat{\text{MP}}_1(\mathbf{X}, \mathbf{A}), \mathbf{A} \right), \mathbf{A} \right). \end{aligned} \quad (20)$$

It is infeasible to fit the data into GPU memory entirely. Instead, we adopt the subsampling strategy in GraphSAGE (Hamilton, Ying, and Leskovec 2017) where we first select a minibatch of nodes and then a subgraph centered around each selected node is obtained by sampling node neighbors with replacement. More specifically, we sample 10, 10 and 25 neighbors at the first, second and third level respectively as DGI. The batchsize of our experiments is 256. Different from transductive setting, we estimate the posterior with pairwise similarities among each minibatch instead of total training set. We set traditional methods DeepWalk and deep learning based methods unsupervised GraphSAGE (Unsup-GraphSAGE), DGI and GMI as baselines. To compare DGCL with supervised counterparts, we report the performance of two representative supervised methods FastGCN (Chen, Ma, and Xiao 2018) and GraphSAGE. More details including hyper-parameters selection can be seen in the appendix.

Table 1: Statistics of datasets used in experiments.

Dataset	Task	Nodes	Edges	Features	Classes
Amazon-Photo	Transductive	7,650	119,081	745	8
Amazon-Computers	Transductive	13,752	245,861	767	10
Coauthor-CS	Transductive	18,333	81,894	6,805	15
Wiki-CS	Transductive	11,701	216,123	300	10
Flickr	Inductive	89,250	899,756	500	7
Reddit	Inductive	231,443	11,606,919	602	41

Table 2: Summary of the accuracies (\pm std) on transductive node classification. The ‘Available Data’ refers to data we can obtain for training, where X , A and Y denotes feature matrix, adjacency matrix and label matrix respectively. ‘OOM’: out of memory on a 32GB V100 GPU. We highlight the performance of DGCL with gray background. The highest performance of unsupervised models is highlighted in boldface; the highest performance of supervised models is underlined.

Method	Available Data	Amazon-Photo	Amazon-Computers	Coauthor-CS	Wiki-CS
Raw features	X	78.53 \pm 0.00	73.81 \pm 0.00	90.37 \pm 0.00	71.98 \pm 0.00
node2vec	A	89.67 \pm 0.12	84.39 \pm 0.08	85.08 \pm 0.03	71.79 \pm 0.05
DeepWalk	A	89.44 \pm 0.11	85.68 \pm 0.06	84.61 \pm 0.22	74.35 \pm 0.06
DeepWalk + features	X, A	90.05 \pm 0.08	86.28 \pm 0.07	87.70 \pm 0.04	77.21 \pm 0.03
GAE	X, A	91.62 \pm 0.13	85.27 \pm 0.19	90.01 \pm 0.17	70.15 \pm 0.01
VGAE	X, A	92.20 \pm 0.11	86.37 \pm 0.21	92.11 \pm 0.09	75.35 \pm 0.14
DGI	X, A	91.61 \pm 0.22	83.95 \pm 0.47	92.15 \pm 0.63	75.35 \pm 0.14
GMI	X, A	90.68 \pm 0.17	82.21 \pm 0.31	OOM	74.85 \pm 0.08
BGRL	X, A	92.58 \pm 0.07	87.65 \pm 0.10	92.72 \pm 0.03	78.35 \pm 0.05
MVGRL	X, A	91.74 \pm 0.01	87.52 \pm 0.11	92.11 \pm 0.12	77.52 \pm 0.08
GCA	X, A	92.45 \pm 0.11	87.60 \pm 0.20	92.44 \pm 0.11	78.03 \pm 0.03
DGCL-weight	X, A	93.27 \pm 0.11	89.14 \pm 0.06	93.43 \pm 0.03	78.26 \pm 0.01
DGCL-mix	X, A	93.41 \pm 0.04	89.33 \pm 0.02	93.45 \pm 0.01	78.08 \pm 0.04
GCN	X, A, Y	92.42 \pm 0.22	86.51 \pm 0.54	<u>93.03 \pm 0.31</u>	77.19 \pm 0.12
GAT	X, A, Y	<u>92.56 \pm 0.35</u>	<u>86.93 \pm 0.29</u>	92.31 \pm 0.24	<u>77.65 \pm 0.11</u>

Datasets

We conduct experiments on six widely-used datasets, including Amazon-Photo, Amazon-Computers, Wiki-CS, Coauthor-CS, Reddit and Flickr. Further information on the datasets can be found in Table 1. To keep fair, for transductive tasks, we split Amazon-Photo, Amazon-Computers, Wiki-CS and Coauthor-CS for the training, validation and testing following (Zhu et al. 2021b; Mernyei and Cangea 2020). For inductive task, we split Reddit and Flickr following (Velickovic et al. 2019; Zeng et al. 2019).

Experimental Results

For transductive classification, as can be observed in Table 2, DGCL consistently performs better than previous unsupervised baselines or even the supervised baselines, which validates the superiority of our DGCL. We provide more observations as following. Firstly, traditional methods node2vec and DeepWalk only using adjacency matrix outperform the simple logistic regression classifier that only uses raw features (“Raw features”) on some datasets (Amazon datasets). However, the latter can perform better on Coauthor-CS and Wiki-CS. Combining the both (“DeepWalk + features”) can bring significant improvements. Compared with GCA,

Table 3: Summary of the micro-averaged F_1 scores (\pm std) on inductive node classification.

Method	Available Data	Flickr	Reddit
Raw features	X	20.3	58.5
DeepWalk	A	27.9	32.4
Unsup-GraphSAGE	X, A	36.5	90.8
DGI	X, A	42.9 \pm 0.1	94.0 \pm 0.1
GRACE	X, A	48.0 \pm 0.1	94.2 \pm 0.0
GMI	X, A	44.5 \pm 0.2	94.8 \pm 0.0
DGCL-weight	X, A	49.4 \pm 0.4	95.0 \pm 0.1
DGCL-mix	X, A	49.6 \pm 0.1	95.3 \pm 0.0
FastGCN	X, A, Y	48.1 \pm 0.5	89.5 \pm 1.2
GraphSAGE	X, A, Y	<u>50.1\pm1.3</u>	<u>92.1\pm1.1</u>

our DGCL emphasize the hard negatives or remove sampling bias, which lifts the representation quality. Secondly, DGCL-mix performs better than DGCL-weight in general because the former considers both hard negatives and removing sampling bias simultaneously while DGCL-weight only removes sampling bias. For inductive tasks, DGCL also obtain competitive performance over other baselines.

Ablation Study

In this section, we replace or remove various parts of DGCL to study the impact of each component.

Table 4: Comparison between BMM and GMM.

Datasets	Amazon-Photo		Amazon-Computers		Coauthor-CS	
Scheme	weight	mix	weight	mix	weight	mix
GMM	92.68	92.89	88.12	89.17	92.88	92.97
BMM	93.27	93.41	89.14	89.33	93.43	93.45

BMM vs. GMM. We replace BMM in our DGCL with GMM and report the performance in Table 4. As can be observed, DGCL equipped with BMM consistently outperforms GMM in both weight and mix schemes. The reason is that BMM can fit the negative samples distribution better than GMM, which has been shown in Figure 3.

Table 5: Comparison between DGCL, DCL, HCL, Ring and MoChi. Here DGCL refers to DGCL-mix. “↑” and “↓” refer to performance improvement and drop compared with GCA respectively.

Methods/Datasets	Amazon-Photo	Amazon-Computers	Coauthor-CS
GCA	92.45	87.60	92.44
+DCL	91.02 (↓ 1.43)	86.58 (↓ 1.02)	92.36 (↓ 0.08)
+HCL	91.48 (↓ 0.97)	87.21 (↓ 0.39)	93.06 (↑ 0.62)
+MoChi	92.36 (↓ 0.09)	87.68 (↑ 0.08)	92.58 (↑ 0.14)
+Ring	91.33 (↓ 1.22)	84.18 (↓ 3.42)	91.51 (↓ 0.93)
+DGCL	93.41 (↑ 0.96)	89.33 (↑ 1.73)	93.45 (↑ 1.01)

DGCL vs. Negative mining and debiased techniques.

To study whether DGCL can better utilize hard negatives and remove sampling bias in GCL, we equip GCA with DCL (Chuang et al. 2020), HCL (Robinson et al. 2021), Ring (Wu et al. 2021b) and MoChi (Kalantidis et al. 2020) which have achieved immense success in CL. As can be seen in Table 5, these techniques bring minor improvements or performance drop over GCA framework. Instead, DGCL introduce consistent and significant improvements over GCA, which further validates that our DGCL is more suitable for GCL.

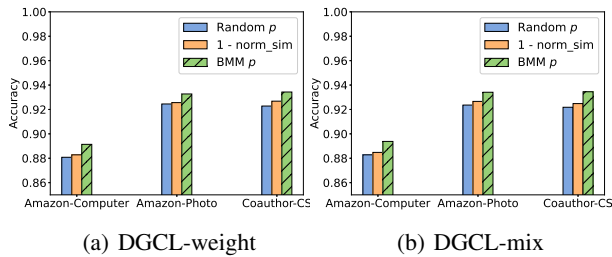


Figure 5: Comparisons among various choices of p (the probability of a sample being true negative).

DGCL p vs. (Random p & tuned p). We substitute the estimated probability p with random p and tuned p (1 - normalized similarity). As can be seen in Figure 5, the tuned p can

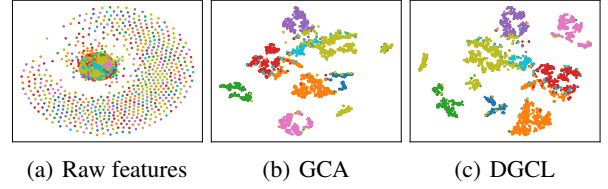


Figure 6: t-SNE embeddings of 2800 nodes randomly selected from Amazon-Photo dataset. Figure 6(a), Figure 6(b) and Figure 6(c) denote raw features, representations learned by GCA model and DGCL respectively. We provide more visualizations in the appendix.

bring minor improvement over random p while the estimated posterior p by BMM is the best among three choices.

Hyperparameters Sensitivity Analysis

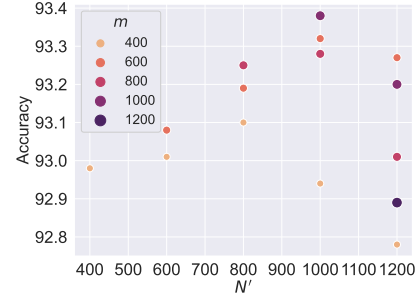


Figure 7: Accuracy when varying N' (x-axis) and m on Amazon-Photo. We study more hyperparameters in the appendix.

Here we study the hyper-parameters of DGCL-mix, i.e., the number of most hard negatives N' and synthetic negatives m . The results shown in Figure 7 illustrate that a large number of samples combinations give consistent performance gains in general. However, oversized N' demonstrated no significant advantages in both accuracy and efficiency. Besides, We provide more details about other hyper-parameters including the epoch E for fitting BMM, the initial weight w_{init} for two components and the iterations I of EM algorithm in the appendix.

Conclusions

In this paper, we unveil the reason why existing techniques that emphasize hard negative samples can not work well in GCL and contrapuntally introduce BMM to fit the negative samples distribution in GCL. In this way, we can probabilistically distinguish the true and false negatives. Moreover, we also devise two schemes to emphasize hard negatives or remove sampling bias, which further boost GCL. Interesting directions of future work include (1) analyzing different data augmentation techniques. (2) exploring the theoretical explanations for the immense success of contrastive learning.

References

- Chen, T.; Kornblith, S.; Norouzi, M.; and Hinton, G. 2020. A simple framework for contrastive learning of visual representations. In *International conference on machine learning*, 1597–1607. PMLR.
- Chen, J.; Ma, T.; and Xiao, C. 2018. Fastgcn: fast learning with graph convolutional networks via importance sampling. *arXiv preprint arXiv:1801.10247*.
- Chuang, C.-Y.; Robinson, J.; Yen-Chen, L.; Torralba, A.; and Jegelka, S. 2020. Debiased contrastive learning. *arXiv preprint arXiv:2007.00224*.
- Everitt, B. S. 2014. Finite mixture distributions. *Wiley StatRef: Statistics Reference Online*.
- Gao, T.; Yao, X.; and Chen, D. 2021. Simcse: Simple contrastive learning of sentence embeddings. *arXiv preprint arXiv:2104.08821*.
- Grover, A., and Leskovec, J. 2016. node2vec: Scalable feature learning for networks. In *Proceedings of the 22nd ACM SIGKDD international conference on Knowledge discovery and data mining*, 855–864.
- Hamilton, W. L.; Ying, R.; and Leskovec, J. 2017. Inductive representation learning on large graphs. *arXiv preprint arXiv:1706.02216*.
- Hassani, K., and Khasahmadi, A. H. 2020. Contrastive multi-view representation learning on graphs. In *International Conference on Machine Learning*, 4116–4126. PMLR.
- He, K.; Zhang, X.; Ren, S.; and Sun, J. 2016. Deep residual learning for image recognition. In *Proceedings of the IEEE conference on computer vision and pattern recognition*, 770–778.
- He, K.; Fan, H.; Wu, Y.; Xie, S.; and Girshick, R. 2020. Momentum contrast for unsupervised visual representation learning. In *Proceedings of the IEEE/CVF Conference on Computer Vision and Pattern Recognition*, 9729–9738.
- Ho, C.-H., and Vasconcelos, N. 2020. Contrastive learning with adversarial examples. *arXiv preprint arXiv:2010.12050*.
- Hu, Q.; Wang, X.; Hu, W.; and Qi, G.-J. 2020. Adco: Adversarial contrast for efficient learning of unsupervised representations from self-trained negative adversaries. *arXiv preprint arXiv:2011.08435*.
- Ji, Y.; Wu, C.; Liu, P.; Wang, J.; and Coombes, K. R. 2005. Applications of beta-mixture models in bioinformatics. *Bioinformatics* 21(9):2118–2122.
- Ji, Z.; Huang, Y.; Xia, Y.; and Zheng, Y. 2017. A robust modified gaussian mixture model with rough set for image segmentation. *Neurocomputing* 266:550–565.
- Kalantidis, Y.; Sariyildiz, M. B.; Pion, N.; Weinzaepfel, P.; and Larlus, D. 2020. Hard negative mixing for contrastive learning. In *Neural Information Processing Systems (NeurIPS)*.
- Kipf, T. N., and Welling, M. 2016a. Semi-supervised classification with graph convolutional networks. *arXiv preprint arXiv:1609.02907*.
- Kipf, T. N., and Welling, M. 2016b. Variational graph auto-encoders. *arXiv preprint arXiv:1611.07308*.
- Lee, D. B.; Min, D.; Lee, S.; and Hwang, S. J. 2021. Meta-GMAE: Mixture of gaussian VAE for unsupervised meta-learning. In *International Conference on Learning Representations*.
- Lindsay, B. G. 1995. Mixture models: theory, geometry and applications. In *NSF-CBMS regional conference series in probability and statistics*, i–163. JSTOR.
- Mernyei, P., and Cangea, C. 2020. Wiki-cs: A wikipedia-based benchmark for graph neural networks. *arXiv preprint arXiv:2007.02901*.
- Pan, S.; Hu, R.; Long, G.; Jiang, J.; Yao, L.; and Zhang, C. 2018. Adversarially regularized graph autoencoder for graph embedding. *arXiv preprint arXiv:1802.04407*.
- Peng, Z.; Huang, W.; Luo, M.; Zheng, Q.; Rong, Y.; Xu, T.; and Huang, J. 2020. Graph representation learning via graphical mutual information maximization. In *Proceedings of The Web Conference 2020*, 259–270.
- Perozzi, B.; Al-Rfou, R.; and Skiena, S. 2014. Deepwalk: Online learning of social representations. In *Proceedings of the 20th ACM SIGKDD international conference on Knowledge discovery and data mining*, 701–710.
- Qiu, J.; Dong, Y.; Ma, H.; Li, J.; Wang, K.; and Tang, J. 2018. Network embedding as matrix factorization: Unifying deepwalk, line, pte, and node2vec. In *Proceedings of the eleventh ACM international conference on web search and data mining*, 459–467.
- Robinson, J. D.; Chuang, C.-Y.; Sra, S.; and Jegelka, S. 2021. Contrastive learning with hard negative samples. In *International Conference on Learning Representations*.
- Thakoor, S.; Tallec, C.; Azar, M. G.; Munos, R.; Veličković, P.; and Valko, M. 2021. Bootstrapped representation learning on graphs. In *ICLR 2021 Workshop on Geometrical and Topological Representation Learning*.
- Tschannen, M.; Djolonga, J.; Rubenstein, P. K.; Gelly, S.; and Lucic, M. 2019. On mutual information maximization for representation learning. *arXiv preprint arXiv:1907.13625*.
- Veličković, P.; Cucurull, G.; Casanova, A.; Romero, A.; Lio, P.; and Bengio, Y. 2017. Graph attention networks. *arXiv preprint arXiv:1710.10903*.
- Veličković, P.; Fedus, W.; Hamilton, W. L.; Liò, P.; Bengio, Y.; and Hjelm, R. D. 2019. Deep graph infomax. In *ICLR (Poster)*.
- Wu, Z.; Xiong, Y.; Yu, S. X.; and Lin, D. 2018. Unsupervised feature learning via non-parametric instance discrimination. In *Proceedings of the IEEE Conference on Computer Vision and Pattern Recognition*, 3733–3742.
- Wu, L.; Lin, H.; Gao, Z.; Tan, C.; Li, S.; et al. 2021a. Self-supervised on graphs: Contrastive, generative, or predictive. *arXiv preprint arXiv:2105.07342*.
- Wu, M.; Mosse, M.; Zhuang, C.; Yamins, D.; and Goodman, N. 2021b. Conditional negative sampling for contrastive learning of visual representations. In *International Conference on Learning Representations*.

- Xia, J.; Lin, H.; Xu, Y.; Wu, L.; Gao, Z.; Li, S.; and Li, S. Z. 2021. Towards robust graph neural networks against label noise.
- You, Y.; Chen, T.; Sui, Y.; Chen, T.; Wang, Z.; and Shen, Y. 2020. Graph contrastive learning with augmentations. In Larochelle, H.; Ranzato, M.; Hadsell, R.; Balcan, M. F.; and Lin, H., eds., *Advances in Neural Information Processing Systems*, volume 33, 5812–5823. Curran Associates, Inc.
- Zeng, H.; Zhou, H.; Srivastava, A.; Kannan, R.; and Prasanna, V. 2019. Graphsaint: Graph sampling based inductive learning method. *arXiv preprint arXiv:1907.04931*.
- Zhu, Y.; Xu, Y.; Yu, F.; Liu, Q.; Wu, S.; and Wang, L. 2020. Deep graph contrastive representation learning. *arXiv preprint arXiv:2006.04131*.
- Zhu, Y.; Xu, Y.; Liu, Q.; and Wu, S. 2021a. An empirical study of graph contrastive learning.
- Zhu, Y.; Xu, Y.; Yu, F.; Liu, Q.; Wu, S.; and Wang, L. 2021b. Graph contrastive learning with adaptive augmentation. In *Proceedings of the Web Conference 2021*, 2069–2080.